Available online at www.sciencedirect.com
ScienceDirect
Remote Sensing of Environment 108 (2007) 138–150
Remote Sensing of Environment
www.elsevier.com/locate/rse

Evaluating remotely sensed live fuel moisture estimations for fire behavior predictions in Georgia, USA

Swarvanu Dasgupta *, John J. Qu, Xianjun Hao, Sanjeeb Bhoi

Center for Earth Observing and Space Research, George Mason University, United States

Received 22 October 2005; received in revised form 23 June 2006; accepted 28 June 2006

Abstract

Research has shown that remote sensing techniques can be used for assessing live fuel moisture content (LFMC) from space. The need for dynamic monitoring of the fire risk environment favors the use of fast, site-specific, empirical models for assessing local vegetation moisture status, albeit with some uncertainties. These uncertainties may affect the accuracy of decisions made by fire managers using remote sensing derived LFMC. Consequently, the analysis of these LFMC retrieval uncertainties and their impact on applications, such as fire spread prediction, is needed to ensure the informed use of remote sensing derived LFMC measurements by fire managers. The Okefenokee National Wildlife Refuge, one of the most fire-prone regions in the southeastern United States was chosen as our study area. Our study estimates the uncertainties associated with empirical site specific retrievals using NDWI (Normalized Difference Water Index; $(R_{0.86} - R_{1.24}) / (R_{0.86}+R_{1.24})$) and NDII (Normalized Difference Infrared Index; $(R_{0.86} - R_{1.64}) / (R_{0.86}+R_{1.64})$) that are simulated by coupled leaf and canopy radiative transfer models. In order to support the findings from those simulations, a second approach estimates uncertainties using actual MODIS derived indices over Georgia Forestry Commission stations that provide NFDRS model estimates of LFMC. Finally, we used the FARSITE surface fire behavior model to examine the sensitivity of fire spread rates to live fuel moisture content for the NFDRS high pocosin and southern rough fuel models found in Okefenokee. This allowed us to evaluate the effectiveness of satellite based LFMC estimations for use in fire behavior predictions. Sensitivity to LFMC (measured as percentage of moisture weight per unit dry weight of fuel) was analyzed in terms of no-wind no-slope spread rates as well as normalized spread rates. Normalized spread rates, defined as the ratio of spread rate at a particular LFMC to the spread rate at LFMC of 125 under similar conditions, were used in order to make the results adaptable to any wind-slope conditions. Our results show that NDWI has a stronger linear relationship to LFMC than NDII, and can consequently estimate LFMC with lesser uncertainty. Uncertainty analysis shows that 66% of NDWI based LFMC retrievals over non-sparsely vegetated regions are expected to have errors less than 32, while 90% of retrievals should be within an error margin of 56. In pocosin fuel models, under low LFMC conditions (<100), retrieval errors could lead to normalized spread rate errors of 6.5 which may be equivalent to an error of 47 m/h in no-wind no-slope conditions. For southern rough fuel models, when LFMC <175, LFMC retrieval errors could amount to normalized spread rate errors of 0.6 or an equivalent error of 9.3 m/h in no-wind no-slope conditions. These spread rate error estimates represent approximately the upper bound of errors resulting from uncertainties in empirical retrievals of LFMC over forested regions.
© 2006 Elsevier Inc. All rights reserved.

Keywords: Fire behavior; Live fuel moisture content; FARSITE

1. Introduction

Live fuel moisture content (LFMC) is one of the critical dynamic factors driving fire initiation, burning efficiency and spread. It can be described as the ratio of the moisture weight to the dry weight of live fuel expressed as a percentage: LFMC = (moisture weight / dry matter weight) × 100. LFMC measurements can be used as inputs to estimate spread rate during a wild or a prescribed fire. Rapid real time assessments of LFMC using remote sensing techniques would thus be very valuable in the management of wild and prescribed fires. Various empirical and physical models utilizing optical and thermal infrared measurements have been investigated. Typically, all remote sensing methods have attempted to measure foliage moisture content, which is a sensitive indicator of vegetation water content. Empirical methods exploiting the obvious correlation between vegetation greenness (chlorophyll content) and moisture content have used indices such as the NDVI or its variations, such as relative greenness, to assess vegetation moisture status (e.g. Burgan & Hartford, 1997;

* Corresponding author. Fax: +1 703 993 1993.
E-mail address: sdasgupt@gmu.edu (S. Dasgupta).

0034-4257/$ - see front matter © 2006 Elsevier Inc. All rights reserved.
doi:10.1016/j.rse.2006.06.023

Chuvieco et al., 1999, 2002). Surface temperature (ST) has also been identified as an indicator of vegetation moisture, since vegetation temperature increases in drier plants on account of reduced evapotranspiration (Jackson, 1986). A number of measures utilizing this water stress related thermal characteristic, such as the CWSI, Crop Water Stress Index (Jackson et al., 1981); SI, the Stress Index (Vidal et al., 1994); WDI, the Water Deficit Index (Moran et al., 1994); and the ratio of NDVI to ST (Alonso et al., 1996; Chuvieco et al., 1999), have been found useful. More direct methods for vegetation water estimation have typically utilized signals from liquid water absorption channels in the near infrared (NIR) or shortwave infrared (SWIR) and contrasted them with signals from liquid water insensitive channels in the near infrared (NIR). Several indices based on SWIR and NIR reflectances have been proposed such as NDWI, Normalized Difference Water Index (Gao, 1996); NDII, Normalized Difference Infrared Index (Hardisky et al., 1983); WI, the water index (Peñuelas et al., 1993, 1996, 1997), SRWI, the Simple Ratio Water Index (Zarco-Tejada et al., 2003; Zarco-Tejada & Ustin, 2001); LWCI, the Leaf Water Content Index (Hunt et al., 1987); GVMI, the Global Vegetation water Moisture Index (Ceccato et al., 2002a). The Tasselled Cap "Wetness" index (Kauth & Thomas, 1976) originally defined as the transformation of raw digital values from Landsat bands, has also been evaluated to measure vegetation water (Chuvieco et al., 2002). Transformations of optical bands calibrated to station data have also been investigated (Hao & Qu, 2007-this issue). More recently, the inversion of coupled leaf and canopy radiative transfer (RT) models have offered a more physically based approach to vegetation moisture estimation (Jacquemoud, 1993; Jacquemoud et al., 1995; Zarco-Tejada et al., 2003).

All these latter methods suffer from inherent limitations which cause uncertainties in LFMC assessments. Vegetation indices are proxy estimates of fuel moisture since they depend on the correlation between vegetation greenness and moisture content. This relation between chlorophyll content and moisture content is not always simple and is known to be plant species dependent (Ceccato et al., 2002b). Apart from water stress, variations in chlorophyll content can be caused by the phenological status of the plant, atmospheric pollution, nutrient deficiency, toxicity, plant disease and radiation stress (Larcher, 1995). Moreover NDVI may not be responsive to the full range of live FMC (Gao, 1996; Jackson et al., 2004) since it saturates at intermediate levels of LAI. The NIR–SWIR indices, which are more direct estimators of vegetation moisture, are also not free from uncertainties. Studies (e.g Bowyer & Danson, 2004; Ceccato et al., 2001) have shown that SWIR–NIR based indices relate more to the equivalent water thickness (EWT), the weight of water per unit area, rather than the LFMC, the weight of water per unit weight of dry vegetation. Relationships between NIR–SWIR based indices and water content are stronger at the leaf level and the latter relationship may weaken at the canopy level, where canopy structure parameters may lead to additional uncertainties in moisture content assessments (Bowyer & Danson, 2004). LFMC retrievals using NIR–SWIR indices would thus have associated uncertainties since they cannot fully account for the contribution that biophysical (leaf area index, leaf orientation, leaf size), geometric (solar and view zenith and azimuth angles), background (soil and or non-photosynthetically active vegetation) make to reflectance variability at the canopy level. Difficulties are also expected in retrievals of vegetation water content through the inversion of physical RT models. RT model inversions are computationally expensive and are prone to ambiguity (Combal et al., 2002; Fourty & Baret, 1997) when prior information about various leaf biochemical parameters and leaf and canopy biophysical parameters are unavailable. The unavailability of prior information becomes particularly problematic during rapid real time assessments using RT inversions. The need for lower latency in monitoring the dynamic fire risk environment thus favors the use of fast, site-specific empirical models for assessing local vegetation moisture status albeit with some uncertainties. Analysis of the range of these uncertainties under site specific conditions and their impact on fire spread rates is necessary to ensure the informed use of remote sensing derived live fuel moisture content in planning and management of forest fires.

This study is focused on the fire prone Okefenokee National Wildlife Refuge (NWR) in Georgia, USA where LFMC estimations would be very useful for fire management. The objectives of this study were to (i) estimate expected uncertainty ranges in empirical estimations of LFMC using NIR–SWIR spectral indices in the Okefenokee and (ii) analyze the implications of these uncertainties for fire spread rate predictions.

2. The okefenokee national wildlife refuge

The Okefenokee National Wildlife Refuge is located on the border of southeast Georgia and northeast Florida and lies within the South Atlantic Coastal Plain (Fig. 1). The refuge encompassing 395,080 acres of the 438,000 acre Okefenokee Swamp is managed by the U.S. Fish and Wildlife Service (USFWS). Designated as a National Wilderness Area, it provides habitats for a wide variety of flora and fauna, including some endangered and threatened species. The primary habitat types are cypress stands (pond cypress, bald cypress), shrub swamps (e.g. fetterbush, dahoon holly, pepperbush), blackgum

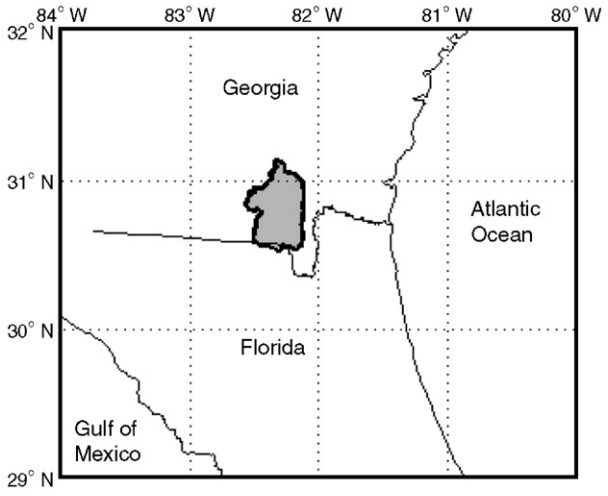

Fig. 1. Location of Okefenokee National Wildlife Refuge.

forests, bay forests (e.g. loblolly bay, red bays, sweet bays) and prairies.

The subtropical climate in the Okefenokee Swamp is characterized by hot and humid summers and cool winters. Despite a humid climatic condition, fires occur frequently in the swamp with the fire occurrence rate classified as "high" by the Forest Service (1969). Fires have been recognized as an important mechanism of the dynamics of the Okefenokee ecosystem, helping to maintain a healthy age composition for vegetation, retarding the natural process of vegetation succession (Cypert, 1961; Duever, 1971) and reducing fuel loads. Moreover fires in the swamp can release a large amount of nutrients and may be an important link in the swamp's nutrient cycle (Yin, 1993). The cause of fires in the Okefenokee Swamp include lightning, ignition from nearby off-refuge fires, careless and intentional arson and prescribed fires (Yin, 1993), the latter becoming increasingly important as instruments of ecosystem management. Trowell (1987) reported that fires in the Okefenokee have occurred in all seasons and areas of the swamp, but major fires tended to occur during the windy spring months in a drought. There have been indications of increased fire activity during the La Niña events when the area becomes drier than normal (Yin, 1993). While analyzing fire records in the Okefenokee from 1938 to 1989, Yin (1993) reported a mean fire size of 1499 ha with a standard deviation of 11,938 ha indicating very large variability in fire size. During the period 2001 to 2004, the USFWS reports a total of 21 wildfires and 56 prescribed fires with total burnt areas around 128,000 acres for wildfires (year 2002 alone accounting for around 118,000 acres) to over 15,000 acres for prescribed fires (http://fire.r9.fws.gov/stats/statistics.htm). The significance of our study is heightened by the intimate link between fire and the region's ecology, especially with current La Niña conditions expected to persist in the near future (http://www.cpc.ncep.noaa.gov/products/analysis_monitoring/enso_advisory/index.html).

3. Experimental methodology

In this study we estimated the expected uncertainty in live FMC measurements in the Okefenokee NWR using empirical models and then assessed the impacts of such uncertainties in predicting fire spread rates. We concentrated on the MODIS instrument aboard the Terra and Aqua platforms, since together they can make two daytime observations, and are thus ideally suited for rapid real time live FMC measurements. Uncertainty estimation was done using two approaches. In the first approach coupled leaf and canopy RT models were used to simulate reflectances in the MODIS NIR–SWIR channels with model parameter ranges set to represent the Okefenokee region. Spectral indices computed from the simulated reflectances were then used to build regression models to retrieve live FMC and determine the uncertainty ranges. In order to reinforce the estimated uncertainty ranges, a second approach was undertaken. Empirical regression models for live FMC retrievals were built by correlating 8 day averaged NFDRS live woody FMC model estimates at Georgia Forestry Commission stations close to the study region with corresponding MODIS 8 day surface reflectance derived spectral indices. These LFMC retrieval models were then analyzed to assess the uncertainty in live FMC retrievals. Finally, to evaluate the effectiveness of satellite based FMC estimations for fire behavior predictions, we examined the sensitivity of fire spread rates to LFMC in the Okefenokee region using the FARSITE surface fire behavior model (Finney, 1998). This was done by perturbing LFMC inputs to FARSITE simulations on site specific fuel models with all other input factors fixed at realistic nominal values.

3.1. Spectral Indices selected for live FMC estimation

Studies have indicated that indices based on liquid water absorption channels are expected to be better estimators of vegetation water content, unlike proxy measures such as vegetation indices or surface temperature. For example Dennison et al. (2005), while analyzing LFMC data measured by the Los Angeles County Fire Department found that NDWI was better correlated to LFMC than NDVI. In this study we have selected the normalized difference water index (NDWI) (Gao, 1996) and the normalized difference infrared index NDII (Hardisky et al., 1983) to represent liquid water absorption based measures. NDWI calculated as $(R_{0.86} - R_{1.24}) / (R_{0.86} + R_{1.24})$ is a normalized index using a weak liquid water absorption 1.24 μm band and the liquid water insensitive 0.86 μm band. The NDII is similar to NDWI except that it uses the relatively stronger 1.64 μm liquid water absorption band instead of the 1.24 μm band.

3.2. Uncertainty estimation using coupled leaf canopy models

The leaf and canopy radiative transfer models used in this study were respectively PROSPECT and GeoSAIL. The well known and validated leaf radiative transfer model PROSPECT (Jacquemond & Baret, 1990) describes the leaf as a stack of elementary plates having particular absorbing and scattering properties. The model version used here (Jacquemoud et al., 2000) simulates leaf reflectance and transmittance as a function of four input parameters: (i) the leaf structure parameter (N) representing the number of elementary layers, (ii) the chlorophyll a and b content (C_{ab}, μg/cm^2), (iii) the equivalent water thickness (EWT, g/cm^2 or cm^{-1}) and (iv) the dry matter content (C_m, g/cm^2) of the leaf. Since live FMC is the percentage weight of water per unit dry matter weight, it can be estimated from EWT and C_m as FMC = (EWT / C_m)×100 (Riano et al., 2005). The PROSPECT simulated leaf optical properties can then be coupled to the inputs of a canopy reflectance model to simulate canopy reflectance. In this study, GEOSAIL (Huemmrich, 1995, 2001), which combines the turbid medium model SAIL (Verhoef, 1984) with Jasinki's geometric–optics model (Jasinski & Eagleson, 1989, 1990), was used to simulate scene reflectance as viewed from nadir. The SAIL component is a turbid medium model which calculates canopy reflectance from inputs of canopy LAI, leaf angle distribution (LAD), leaf and soil optical properties and the solar and sensor illumination and viewing geometries. The geometric optics component of GEOSAIL computes the

Table 1
Input parameter ranges for radiative transfer simulations

Variable	Range
Live leaf fuel moisture content (LFMC) (%)	50–200
PROSPECT	
Chlorophyll concentration (C_{ab}, μg/cm^2)	35 (fixed)
Structural parameter (N, dimensionless)	1–4
Dry matter content (C_m, g/gm^2)	0.0033–0.0111
Equivalent water content (EWT, g/cm^2)	Computed from C_m and LFMC values as EWT = (LFMC × C_m)/100
GEOSAIL	
Canopy leaf area index (LAI)	3–9
Leaf angle distribution (LAD)	Uniform
Fractional vegetation cover (Fcov)	0.8–1.0
Height to width ratio (h/w)	2–3
Canopy shape	Cone
Background reflectance	Dry or wet (see Table 2)
Solar zenith angle (SZA)	15°–55°

fractional area of scene constituents (sunlit canopy, shaded canopy, sunlit background and shaded background) using additional inputs of fractional vegetation cover (Fcov), canopy crown shape and crown height to width (h/w) ratio. The total nadir scene reflectance is then simulated as the linear combination of reflectance from each scene constituent weighted by their fractional area.

3.2.1. PROSPECT and GeoSAIL input parameter ranges

In order to simulate site-specific reflectances, we restricted the PROSPECT model to characteristic parameter ranges. Since we were simulating MODIS NIR and SWIR bands at 0.86, 1.24 and 1.64 μm, the chlorophyll concentration parameter C_{ab} was kept fixed at 35 μg/cm^2 for our simulations. This parameter has been proved to have no effect on NIR−SWIR wavelengths (Ceccato et al., 2002a). The leaf dry matter content C_m has been shown to be species dependent with considerably less within species variance than inter-species variance (Riano et al., 2005; Shipley & Vu, 2002). Mitchell et al. (1998) intensively sampled eighteen tree species that were prevalent in southeastern United States and estimated their Specific Leaf Area (SLA cm^2/gm; SLA = 1 / C_m) ranges. SLA ranges from eleven of those species which are found in Georgia's coastal plain (Bishop, 2000) were used to construct a dry matter content range (C_m) representative of the Okefenokee. The structural parameter N relates to the cellular arrangement within the leaf, but is not a measurable physical quantity. Jacquemond & Baret (1990) mentions the range of N to vary between 1 to 1.5 and 1.5 to 2.5 for monocotyledons and dicotyledons respectively, with N values greater than 2.5 representing senescent leaves. Ceccato et al. (2001) used the PROSPECT model along with leaf optical and biochemical properties from LOPEX93 dataset to conclude that N normally ranges from 1 to 4. Based on the above findings our simulations used the same N range (1–4). The EWT parameter was computed from LFMC and C_m using EWT = (LFMC × C_m) / 100 with LFMC restricted to vary between its normal range of 50 to 200 (Bradshaw et al., 1984). LFMC exceeds 100 when the liquid water weight in the fuel exceeds the dry matter weight in the fuel. All the parameter ranges are specified in Table 1.

GEOSAIL parameter ranges were also set so as to be applicable to the study region (Table 1). Using typical values for forested regions (Myneni et al., 1997), fractional vegetation cover (Fcov) was allowed to vary from 0.8 to 1.0, and LAD was set as a uniform distribution. Canopy LAI range of 3 to 9, was considered suitable for the primarily evergreen forests of Okefenokee. NIR–SWIR indices have been shown to perform poorly in sparsely vegetated canopies where soil reflectance contaminates the vegetation moisture information in the canopy signal (Ceccato et al., 2002a; Gao, 1996). Indeed this limitation should not pose a major problem in densely vegetated areas such as the Okefenokee. Note that with Fcov ranging from 0.8 to 1.0 and canopy LAI from 3 to 9, the average LAI over the whole scene (or pixel) ranges from 2.4 (= 3 × 0.8) to 9. The crown shape, height and width of 6 predominant woody tree species in Okefenokee (Bald Cypress, Blackgum, Loblolly Bay, Red Bay, Sweetbay Magnolia, Red Maple) were looked up (http://www.ces.ncsu.edu/depts/hort/consumer/factsheets/trees-new/index.html) to fix the crown shape as conical and the height to width ratio as ranging from 2 to 3. In absence of litter and soil reflectance measurements at Okefenokee, representative reflectances from broadleaf litter and ultisol soil (also found in Okefenokee) measured by Nagler et al. (2000) were found appropriate to characterize the background variability. Reflectance from dry and wet broadleaf litter and wet ultisol soil at 0.86 μm and 1.64 μm were obtained from Nagler et al. (2000) and corresponding reflectances at 1.24 μm were obtained by linear interpolation between the two latter wavelengths. In order to account for background reflectance variability in our simulations, canopy background was set as either "dry" or "wet" (Table 2). Reflectance from a "dry" background was considered to be a linear mixture of reflectances from dry litter and wet soil in equal proportions. Similarly, reflectance from a "wet" background was assumed to be a linear mixture of reflectances from wet litter and wet soil in equal proportions. The soil component was always assumed to be wet, keeping in mind that Okefenokee is a swamp. Solar zenith angle was set to vary between 15° and 55° representing the approximate range while observing Okefenokee from the Terra and Aqua platforms.

Values for LFMC and each leaf and canopy structure parameters except EWT was randomly generated within their predetermined site specific ranges (Table 1). For each such combination the equivalent water thickness (EWT) parameter was calculated as EWT = (LFMC × C_m) / 100. A set of 1000 input combinations thus generated was utilized by the coupled PROSPECT–GeoSAIL models to simulate a set of 1000 canopy reflectances. Spectral indices computed from the

Table 2
Background reflectance used in reflectance simulations

Background	0.86 μm	1.24 μm	1.64 μm
Wet background (50% wet litter and 50% wet soil)	0.230	0.255	0.280
Dry background (50% dry litter and 50% wet soil)	0.260	0.320	0.380

simulated reflectances after correction for solar zenith angle effects were then used to build regression models to retrieve live FMC and quantify the uncertainty ranges using measures of mean absolute errors and prediction intervals (confidence intervals for predictions).

3.3. Uncertainty estimation using NFDRS model live woody FMC and MODIS reflectances

In this second approach to determine expected errors in LFMC retrievals, live woody fuel moisture estimated using US National Fire Danger Rating System (NFDRS) models was correlated with corresponding MODIS spectral indices. These modeled live woody FMC values were provided by the Georgia Forestry Commission over various RAWS (Remote Automated Weather Stations) sites on a daily basis. Three stations namely Camilla (31.21N, 84.24W), Waycross (31.25N, 82.40W) and Midway (31.78N, 81.44W) situated in the South Atlantic coastal plain and close to the Okefenokee were chosen for this analysis. A basic overview of the NFDRS live woody fuel moisture model would be pertinent at this stage.

3.3.1. NFDRS live woody fuel moisture model

The NFDRS classifies forest fuels into dead and live varieties and provides modeled estimates of fuel moisture content (FMC) of these fuels based on environmental conditions at different US sites. Live fuels are classified into herbaceous (grasses, ferns etc) and woody (leaves and small twigs of woody plants) types. Moisture content in live fuels is controlled by the physiological processes of the plant (Bradshaw et al., 1984) and is much less dependent on environmental conditions since living plants can extract water from the soil reserve and reduce evapotranspiration. Moisture content in dead fuels on the other hand is exclusively controlled by environmental conditions such as temperature, radiation, relative humidity, wind and precipitation and is modeled from these parameters in the NFDRS (Rothermel et al., 1986). Dead fuel is classified into 1 h (hour), 10 h and 100 h and 1000 h classes depending on the time required to lose approximately two-thirds of their initial moisture content under constant conditions (Bradshaw et al., 1984). Among dead fuels, the moisture content in 1000 h dead fuels (dead wood with diameters between 3 to 8 in.) is least affected by environmental conditions and their response to wetting and drying cycles is very similar to live fuels. Thus the 1000 h timelag fuel moisture content serves as the basic meteorological factor for modeling live woody fuel moisture content in the NFDRS. The 1000 h dead fuel moisture model uses daily measurements of maximum and minimum air temperatures and relative humidity during the last 7 days to predict the current 1000 h dead fuel moisture. The modeled 1000 h dead fuel moisture is then used along with climate class dependent coefficients and greenness factors to predict the current live woody FMC (Burgan, 1979, 1988). The NFDRS describes four climate classes for the United States depending on broadscale plant moisture responses; the Okefenokee region falling under the humid climate class. During the dormant winter periods the described model is not applied. Instead a constant climate class specific minimum is used. The live woody FMC model has been an important part of NFDRS for decades and has been used by US Forest Service to assess fire danger across the country (San-Miguel-Ayanz et al., 2003). The 1988 revisions to the NFDRS (Burgan, 1988) were geared towards providing better live woody FMC estimates for the humid conditions in southeast and northeast USA. Remote sensing based LFMC retrievals over forested regions are expected to estimate fuel moisture content in the live woody fuel classes since live herbaceous and dead fuels are more likely to be hidden under the canopy. Since our primary interest in this paper is the retrieval of live woody FMC, henceforth live woody FMC and LFMC would be used interchangeably.

We built regression models using NFDRS live woody FMC estimates along with coincident Aqua MODIS spectral indices. Georgia Forestry commission provides daily estimates of live woody FMC over the stations at 1.30pm EST which is around the overpass time of Aqua (1pm local time). Daily live woody FMC model data from March 22nd 2005 to November 16th 2005 (covering spring, summer and autumn) were acquired from the Georgia Forestry Commission Weather/NFDRS data Retrieval System at http://weather.gfc.state.ga.us/Getwxdata/Getwxdata.aspx. Values before March 22nd were not considered since they represent the dormant period when the live woody FMC is held at a constant minimum. In order to minimize possible noise in daily live woody FMC model estimates and improve robustness, we averaged the daily estimates over 8 day periods (total of 30 8-day periods). The standard deviation within each 8 day period was also computed as a measure of variability of live woody FMC during that period. We also acquired MODIS Aqua 8 day surface reflectance products over the region during the same temporal period (March 22nd 2005 to November 16th 2005 for a total of 30 reflectance datasets). The MODIS/Aqua Surface Reflectance 8-Day L3 Global 500 m SIN Grid product, MYD09A1, is a composite of the previous 8 daily L2G Surface Reflectance products (MYD09GHK). This MODIS product provides estimates of the surface spectral reflectance for each solar reflectance band (bands 1–7) as it would be measured at ground level in the absence of atmospheric scattering or absorption. The MODIS products were resampled to a resolution of 0.01° (~1 km^2) to reduce residual mis-registrations and corrected for solar zenith angle effects. NDWI and NDII values were then computed for the 1 km^2 pixel associated with each of the 3 stations on each of the 30 observation periods for a total of 90 values. The MODIS 8 day product is not an 8 day averaged surface reflectance. Rather, the best observations during an 8 day period, as determined by overall pixel quality and observational coverage, are matched geographically. Thus the 8 day surface reflectance and the 8 day averaged NFDRS live woody FMC estimates may not represent the same observation unless the live woody FMC during that 8 day period remains stable with no significant variability. Based on this argument, the 8 day averages with corresponding standard deviation $\sigma > 5$ (average standard deviation of live woody FMC within 8 day periods was around 5) were considered to have significant variability and were discarded from the analysis. Further, satellite observations over the

selected stations having scan angles greater than 30° were not considered for deriving the regression equation since larger pixel sizes at such scan angles would deteriorate the validity of the regressed equation. Such a scan angle restriction would also limit effects of surface anisotropies on reflectances. Finally out of a possible 90 NFDRS live woody FMC and Aqua NDWI, NDII pairs, only 24 of them survived the scan angle and live woody FMC standard deviation filtering. These 24 pairs were used to build the linear regression models and determine the potential uncertainties in LFMC retrievals.

3.4. Estimating sensitivity of fire behavior to live woody FMC

Errors in empirical LFMC estimations using the NDWI and NDII indices may lead to erroneous predictions of fire spread rate. The effectiveness of LFMC retrievals, with their inherent uncertainties, was evaluated by examining the sensitivity of fire spread estimates to live woody FMC. The sensitivity analysis was done using the FARSITE surface fire spread model (Finney, 1998). Errors in fire spread rate computations for unit errors in LFMC retrievals were quantified for site specific simulations of fire spread.

3.4.1. The FARSITE fire spread model

The surface fire spread rate model used in the FARSITE is the well-known Rothermel spread equation (Rothermel, 1972). The steady state fire spread rate (m/min) in a plane parallel with the ground surface at any point on a landscape is given as.

$$R = R^0(1 + \Phi_w + \Phi_s) \quad (1a)$$

where

$$R^0 = (I_p)_0/(\rho_b \varepsilon Q_{ig}) \quad (1b)$$

Here R_0 is the no-wind no slope fire spread rate. In the denominator Qig (kJ/kg) is the pre-ignition heat energy of the fuel, p_b (kg/m^3) is the actual fuel ovendry bulk density, ε is the effective heating number (dimensionless). In the numerator $(I_p)_0$ (kJ/m^2 − min) is the heat flux absorbed by a unit volume of fuel at the time of ignition under no wind and no slope conditions. Under wind and slope conditions the no-wind no slope spread rate must be modified by multiplying it by the term $(1+\Phi_w+\Phi_s)$. Φw and Φs represent the additional radiative and convective flux that the fuel is exposed to due to wind and slope respectively. They are dimensionless coefficients depending on wind, slope and fuel models. The rate of spread in Eq. (1a) in a sense is a ratio between heat flux received from the source (heat source) in the numerator and the heat required for ignition by the potential fuel (heat sink) in the denominator. Fire spread rate as expected is inversely proportional to fuel moisture content. Fire growth modeling in FARSITE is carried out using a vector approach as described in Richards (1990, 1993). FARSITE requires five raster layers of fuel model, slope, aspect, elevation and percentage vegetation cover as input. Other inputs include daily observations of maximum and minimum temperature and relative humidity, precipitation duration, cloud cover, latitude of the region and the dates for the simulation. Fuel moisture inputs include initial fuel moistures of 1 h, 10 h, 100 h dead fuels, and herbaceous and woody live fuel for each fuel model within the landscape. Weather inputs and the estimated solar radiation are used to model the changes in dead fuel moisture over the course of the fire simulation period. The live fuel moisture content remains invariant over the simulation period.

3.4.2. FARSITE simulations

The GTOPO30 DEM dataset from US Geological Survey provides global elevations with horizontal grid spacing of 30 arc seconds (approximately 1 km). Analysis of this dataset over the Okefenokee revealed (Fig. 2a) that the refuge is essentially a flatland (median 36 m; σ = 4 m.) For fuel model distribution we used the NFDRS fuel model (Bradshaw et al., 1984; Burgan, 1988) dataset from Wildland Fire Assessment System (WFAS, http://www.fs.fed.us/land/wfas/nfdr_map.htm) operated by the National Interagency Fire Center (NIFC), Boise, Idaho. NFDRS fuel models have been mapped across the lower 48 states at 1 km resolution. Although fire behavior models typically use the 13 fuel models described by Anderson (1982), what they essentially require are descriptions of fuel parameters such as fuel loading, heat content,

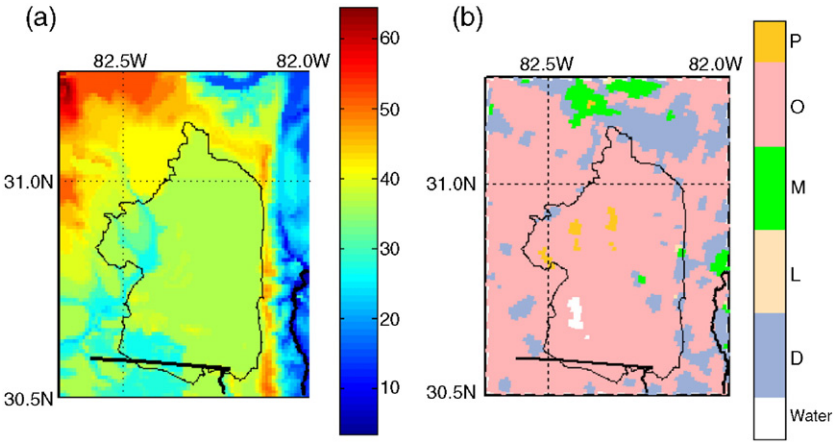

Fig. 2. (a) Elevation in meters using GTOPO30 DEM dataset and (b) NFDRS fuel model using data from the Wildfire Assessment System for the Okefenokee National Wildlife Refuge. The elevation distribution shows that Okefenokee area does not have much topography (mean elevation=36 m σ=4 m). The predominant fuel models are fuel model O (high pocosin, ~88% of area) and fuel model D (southern rough, ~10% of area).

Table 3
Primary fuel models in Okefenokee and their parameters

Fuel model	Fuel loading (tons/acre)					Surface area to volume (ft^{-1})			Fuel bed depth (ft)	Dead fuel moisture of extinction (%)	Heat content (all fuels) Btu/lb
	1 h	10 h	100 h	Live woody	Live herb.	1 h	Live woody	Live herb.			
High pocosin (O)	2.0	3.0	3.0	7.0	–	1500	1500	–	4.0	30	9000
Southern rough (D)	2.0	1.0	–	3.0	1.0	1250	1500	1500	2.0	40	9000

and surface area to volume ratio, fuel bed depth, and dead fuel moisture of extinction, all which can also be provided by the NFDRS fuel model. The NFDRS fuel model distribution for the Okefenokee region (Fig. 2b) shows that two fuel models viz — fuel model O (high pocosin, ~88% of area) and fuel model D (southern rough, ~10%) cover almost 98% of the refuge. Fuel parameters pertaining to fuel models D and O (Burgan, 1988) are given in Table 3. The O fuel model applies to dense brushlike fuels of southeastern US, while fuel model D is specifically for the palmetto–gallberry understory pine overstory association of the southeast coastal plains. In order to quantify the sensitivity of fire spread rates to live woody FMC over these two predominant fuel models, two experimental landscapes were constructed. The two landscapes at latitude 31°N were modeled to be flat (no slope, constant elevation of 36 m), with a constant canopy cover of 0.9 and a constant fuel model of either high pocosin or southern rough. Repeated fire spread simulations were performed on these experimental landscapes for 8 daylight hours between 8am to 4pm on a typical summer day by perturbing the live woody FMC values for each simulation and keeping all the other factors fixed. The temperature and relative humidity were set respectively to the 75th percentile (~85 °F) and the 25th percentile (~45%) of daily air temperature and relative humidity observations at the 3 Georgia Forestry Commission stations during 2005. Similarly moisture content in the 1 h, 10 h 100 h dead fuel classes and the live herbaceous classes were set to the 25th percentile of corresponding NFDRS model observations at the same sites during 2005. The air temperature, relative humidity and fuel moisture of the dead and the live herbaceous classes used in our experiments can thus represent realistic high burning conditions characteristic of the Okefenokee. Winds over the landscape were kept at zero during our simulations. The simulation conditions are given in Table 4. Similar experimental simulations on the BEHAVE fire behavior model (Andrews, 1986) were used by Dimitrakopoulas (2002), to determine the indicative range of spread rates on different fuel models in Greece.

3.4.3. Normalized spread rates

Fire simulations in the homogenous landscapes (flat with constant fuel models) under the constructed weather conditions were not meant to predict actual fire behavior over the Okefenokee since that would require high resolution inputs of fuel model and topography as well as accurate spatial and temporal descriptions of the weather. However, our experimental simulations should be adequate to determine the no-wind no-slope fire spread rates R_0 (m/min) in the two predominant fuel models. These no-wind no-slope fire spread rates R_0 can be extended for slope and wind conditions by multiplying them by a factor $(1+\Phi_w+\Phi_S)$ (Refer Eq. (1a)). The wind and slope coefficients Φ_w and Φ_S are fuel model dependent and can be computed from wind speed and slope respectively. Further, the fire spread rates predicted by FARSITE are approximate estimates applicable for the broad fuel model classes and may sometimes need to be further tuned to the local region by multiplying them with appropriate fuel model specific adjustment factors (Finney, 1998). For example, an adjustment factor of 0.5 reduces the spread rate by half, while an adjustment factor of 2.0 doubles the spread rate. In short, all the wind, slope and regional adjustments required to determine the actual fire spread rate appear as fuel moisture independent multiplicative terms to the no-wind no-slope spread rate. Thus a ratio of spread rates at two different live woody fuel moistures on the same fuel model is independent of any wind, slope and regional adjustments. For example let the spread rate at a live woody FMC of 75 be $R_{75} = R^0_{75}(1+\Phi_w+\Phi_S)a$, where a is the local adjustment factor and R^0_{75} is the no-wind no-slope spread rate predicted by FARSITE for LFMC of 75. The spread rate at a live woody FMC of 125 under the same conditions would then be $R_{125} = R^0_{125}(1+\Phi_w+\Phi_S)a$, where R^0_{125} is the no-wind no slope spread rate predicted by FARSITE for LFMC of 125. The ratio of these two spread rates $R_{75} / R_{125} = [R^0_{75}(1+\Phi_w+\Phi_S)a] / [R^0_{125}(1+\Phi_w+\Phi_S)a] = R^0_{75} / R^0_{125}$ would thus be independent of wind-slope and regional adjustment factors. Based on this observation, we describe a normalized spread rate at a live woody FMC of n as $R^*_n = R_n / R_{125}$; where R_n and R_{125} are the spread rates at live woody FMC of n and 125 under the same conditions. The normalized spread rate at a LFMC of n is interpreted as the factor by which the actual spread rate at LFMC of n is faster or slower than the actual spread rate at LFMC of 125 in the same fuel model and under the same slope and wind conditions ($R_n = R^*_n \times R_{125}$). The most important property of the normalized spread rate is that it is wind, slope and adjustment factor invariant and can be easily computed from our no-wind no-slope simulations, since $R_n / R_{125} = R^0_n / R^0_{125}$. Our sensitivity results would be presented both in terms of the no-wind no-slope non adjusted fire spread rates, as well as the normalized spread rates. The use of normalized spread rates for quantifying the sensitivity are intended to make our results adaptable to different wind, slope conditions as

Table 4
Farsite simulation conditions

Variable	Nominal value
1 h and 10 h dead FMC (%)	8
100 h dead FMC (%)	8
Live herbaceous FMC (%)	15
Temperature (°F)	85
Relative humidity (%)	45
Wind speed (m/h)	0
Rainfall	Nil
Cloud cover (%)	0

well as any localized adjustments that may be required. Fire managers who are generally aware of the actual spread rates at average conditions (LFMC of 125) would be able to easily adapt the results to the actual situation.

4. Results and discussion

4.1. Uncertainty estimation using coupled leaf canopy models

Reflectances at wavelengths 0.86 μm, 1.24 μm and 1.64 μm corresponding to MODIS bands 2, 5, and 6 were simulated by the coupled PROSPECT–GEOSAIL model with input parameters set to site specific ranges. These simulated reflectances were used to compute NDWI and NDII. Live FMC for each simulated reflectance was the ratio of corresponding model input parameters of equivalent water content (EWT) and dry matter content (C_m) multiplied by 100; i.e. LFMC = (EWT / C_m) × 100.

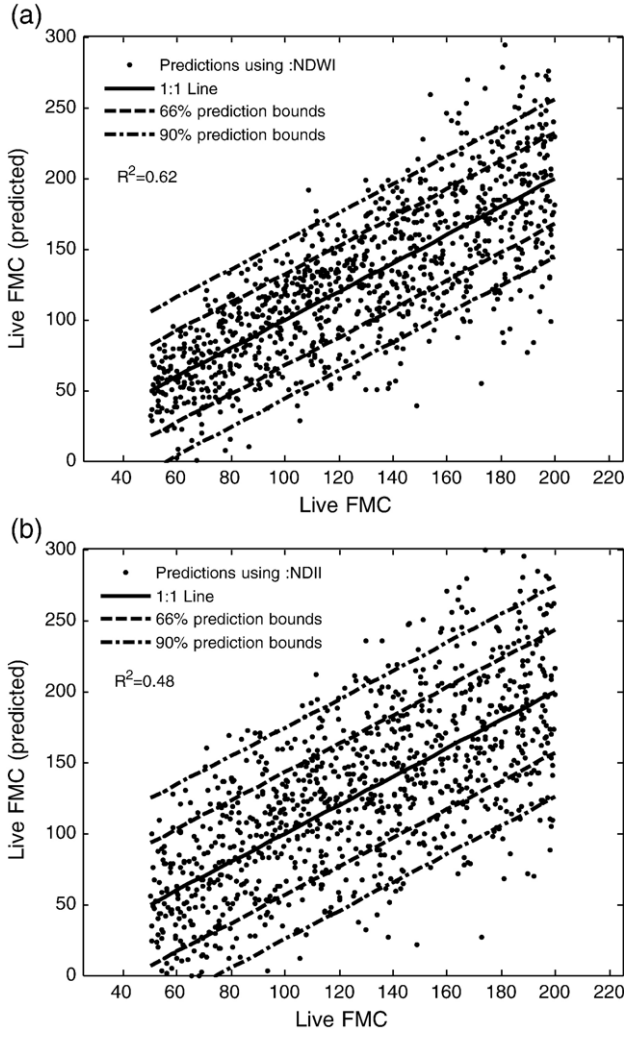

Fig. 3. Actual vs predicted LFMC using (a) simulated NDWI and (b) simulated NDII. NDWI and NDII was simulated using coupled PROSPECT and GeoSAIL model with site specific input parameter ranges. LFMC was predicted using linear regression models built using simulated NDWI NDII and the input LFMC. All correlations are significant ($p < 0.0001$). Average 66% and 90% prediction error bounds for NDWI based retrievals are 32 and 56. For NDII based retrievals they are 43 and 75.

Table 5
Least square regression for lfmc retrieval

Spectral index used	Regression equation	Mean absolute error	Avg 66% error bounds	Avg 90% error bounds
Simulated NDWI	NDWI = 0.0005794 × LFMC + 0.00571	26.7	32.4	55.9
MODIS NDWI over GFC stations	NDWI = 0.0013 × LFMC − 0.2117	23.8	32.0	56.3
Simulated NDII	NDII = 0.00123 × LFMC + 0.1647	36.1	43.2	74.5
MODIS NDII over GFC stations	NDII = 0.003 × LFMC − 0.2546	28.9	40.1	70.6

The simulated spectral indices and the corresponding LFMC were used to build linear regression models with LFMC as the independent variable and the spectral index as the dependent variable. The inverse models were then used to predict the LFMC. Fig. 3(a) and (b) shows the scatter-plot of the actual LFMC (computed from the model input parameters) and the LFMC predicted from the linear regression models. In order to quantify the uncertainties in model predictions, we employed statistical measures of prediction intervals. The prediction interval at a specified level of LFMC statistically estimates the interval range in which future predictions would lie with a certain degree of confidence (Montgomery et al., 2001). We estimated 66% and 90% prediction intervals at different levels of actual live FMC levels between 50 and 200 at increments of 5 (Fig. 3a and b). Prediction intervals at a confidence level of 66% can be interpreted as the bounds within which on an average 66% of predictions would be expected to lie. A similar interpretation would be applicable to 90% prediction bounds, implying that on average 90% of predictions could be expected within those limits. One half of the length of the prediction intervals would be an estimate of the amount of error expected from the linear regression models with confidence associated with the interval. Table 5 shows these error estimates along with the mean absolute errors for the regression models employing NDWI and NDII. The average 66% and 90% error bounds for NDWI based retrievals are about 32 and 56, while the corresponding values for NDII based retrievals are about 43 and 75. The mean absolute errors for NDWI and NDII based models are estimated as about 27 and 36. NDWI thus seems to be a better estimator of LFMC than NDII. This observation agrees with similar findings from Serrano et al. (2000) who found the WI and the NDWI that used weaker liquid water absorption channels exhibited a stronger correlation and linear relationship to vegetation water than indices such as NDII that used stronger liquid water absorption channels. This better correlation was attributed to the greater canopy penetration and less saturation at the weaker water absorption bands (Peñuelas et al., 1993). Vegetation scattering properties at 0.86 μm are more similar to scattering properties at 1.24 μm (Gao, 1996) than at 1.64 μm, implying that the NDWI can be expected to provide a better normalization of external effects than NDII.

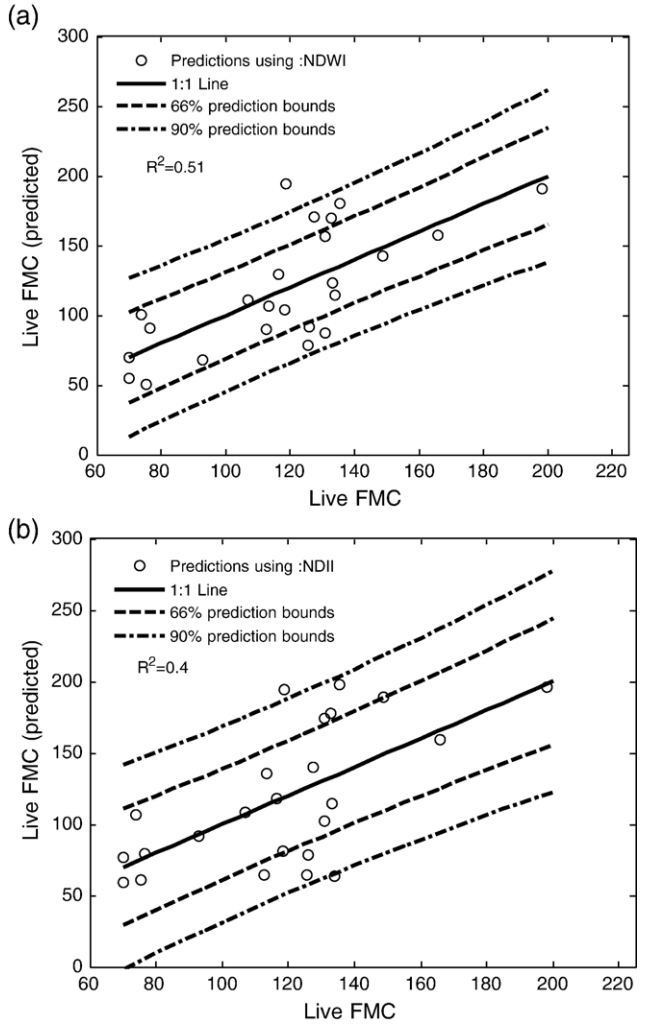

Fig. 4. Actual vs predicted FMC using (a) Aqua MODIS NDWI and (b) Aqua MODIS NDII over Georgia Forestry Commission stations. LFMC were predicted using linear regression models built from NFDRS model live woody FMC values and the corresponding Aqua MODIS derived NDWI and NDII. All correlations are significant ($p<0.001$). Average 66% and 90% prediction error bounds for NDWI based retrievals are 32 and 56. For NDII based retrievals they are 40 and 71.

4.2. Uncertainty estimation using NFDRS model live woody FMC and MODIS reflectances

Linear regression models built from 8 day Aqua MODIS surface reflectance derived spectral indices and 8 day averaged NFDRS model estimates of live woody FMC were also evaluated for uncertainties using prediction intervals. The average 66% and 90% error bounds for LFMC retrievals are 32 and 56 for NDWI based retrievals, and about 40 and 71 for NDII based retrievals (Fig. 4a and b). The mean absolute errors are 24 and 29 for NDWI and NDII based models respectively. The error estimates are very similar to those obtained from the simulation study and reinforce the error estimates obtained from the latter (Table 5). It should be noted here that it may not be feasible to retrieve NDII using Aqua MODIS on a daily basis because there are some non functioning detectors for Aqua MODIS band 6 (Wang et al., 2006). This is expected not be an issue of concern for our study, since we used the Aqua 8 day surface reflectance products which are generated by using the best surface reflectance estimates over the 8 day period.

The R^2 values between predicted and actual LFMC using simulated and real spectral indices range from 0.40 to 0.62. Given the host of biophysical to geometrical factors that serve to confound the relationship between satellite derived indices and live FMC, the R^2 values are quite consistent with expected results. Dennison et al. (2005) reported R^2 values from 0.39 and 0.80 when comparing MODIS derived NDWI with live FMC values collected at different sites within Los Angeles County, California. Bowyer and Danson (2004) found R^2 values of 0.42 and 0.47 between PROSPECT+SAIL and PROSPECT+GeoSAIL simulated NDWI and LFMC under site specific conditions. Peñuelas et al. (1997) reported correlation coefficients between 0.56 and 0.71 between plant water concentration and spectral indices of WI and WI/NDVI. The WI was calculated as the ratio of the reflectances at 0.9 μm and 0.97 μm. In another study Chuvieco et al. 2002 evaluated multiple regression techniques using different Landsat derived spectral indices for retrievals of fuel moisture content in Mediterranean grasslands and shrublands. Average errors of 23.45 to 40 in the estimation of fuel moisture in grasslands were found, depending on which spectral indices were included in the multiple regression. For the fuel moisture estimation in shrub species, average errors were lower (7.94 to 19.4), since the range of fuel moisture values in shrublands were lower.

4.3. Estimating sensitivity of fire behavior to live woody FMC

With these estimates of potential errors in satellite derived LFMC using region specific linear regression methods, we then investigated the implications of these errors for fire behavior predictions. FARSITE simulations on the predominant Okefenokee fuel models at high burning conditions (Table 4) under no wind no slope conditions were used to determine the

Table 6
Sensitivity of fire spread rate to live woody fuel moisture content

Fuel models	LFMC range	Errors in normalized spread rates per unit error in LFMC retrieval	Error in normalized spread rate for error of 32 in LFMC retrieval	Error in normalized spread rate for error of 56 in LFMC retrieval	Errors in no-wind no-slope non-adjusted spread rates per unit error in LFMC retrieval (m/h)	Error in no-wind no-slope non-adjusted spread rate for error of 32 in LFMC retrieval (m/h)	Error in no-wind no-slope non-adjusted spread rate for error of 56 in LFMC retrieval (m/h)
High	≤100	0.1159	3.7	6.5	0.8408	26.9	47.1
pocosin	>100	0.0046	0.15	0.26	0.0332	1.06	1.86
Southern	≤175	0.0113	0.36	0.63	0.1668	5.34	9.34
rough	>175	0.0015	0.05	0.08	0.0223	0.71	1.25

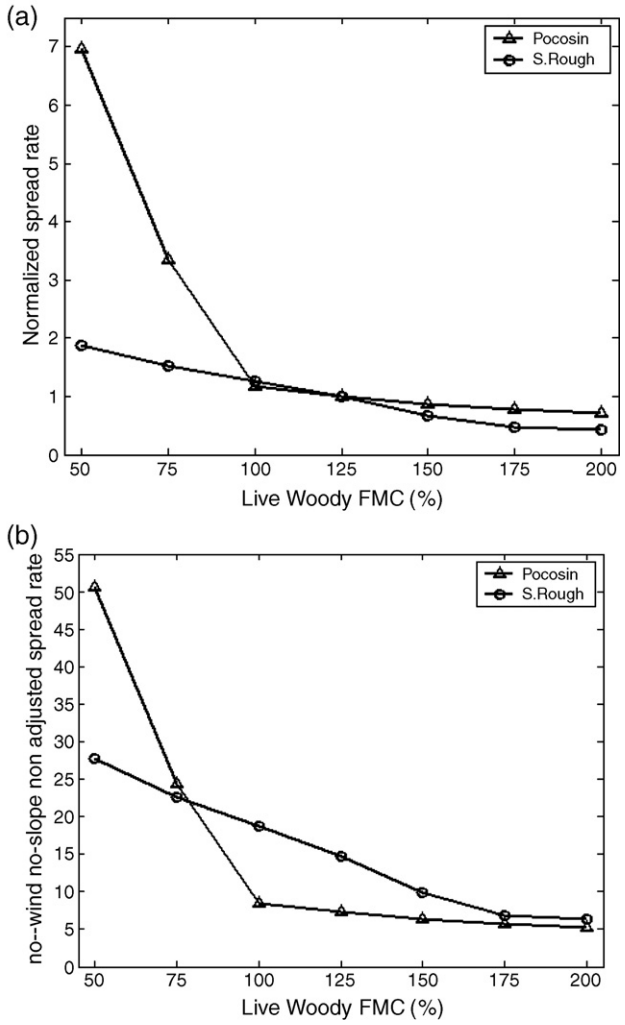

Fig. 5. Effect of live woody FMC on (a) normalized spread rates and (b) no-wind no-slope non adjusted spread rates in fuel models of high pocosin and southern rough.

sensitivities of fire spread rates to live woody FMC. Fig. 5a shows the change in normalized fire spread rates due to change in live woody fuel moisture. By construction, the normalized spread rate at a specified fuel moisture is the factor by which it is faster or slower than the spread rate at fuel moisture of 125 for the same fuel model and under similar environmental and topographical conditions. Normalized spread rates were found suitable for analyzing sensitivity of live woody FMC, since they remain invariant under differing wind and slope conditions, and to any local adjustments that may be needed. Fire managers aware of the actual spread rates under average live woody FMC of 125 would find it easy to adapt the sensitivity results to the actual field situation. The sensitivity of the no-wind and no slope non adjusted spread rates to live woody FMC can be perceived from Fig. 5b. The slopes of the sensitivity curves at different live woody fuel moisture intervals are measures of expected errors in estimating fire spread rates for unit error in live woody FMC retrieval (Table 6). As expected, fire spread rates are inversely proportional to live woody FMC. The sensitivity however decreases with increasing live woody FMC, since with increasing live woody fuel moisture, live fuel becomes more of a heat sink than a heat source (Bradshaw et al., 1984). Sensitivities of fire spread rate to LFMC (change in spread rates per unit change in LFMC) for a LFMC range between $LFMC_i$ and $LFMC_j$ with corresponding spread rates R_i and R_j was determined as $|(R_i - R_j)/(LFMC_i - LFMC_j)|$.

The curves for pocosin fuels (Fig. 5a and b) show two very different regions of sensitivity. Below LFMC of 100 a unit error in LFMC retrieval can lead to an error 0.1159 in normalized spread rates or an equivalent error of 0.84 m/h (meter/hour) in predicting no wind no-slope non-adjusted spread rate. Above a LFMC of 100 in pocosin fuels, the sensitivity decreases considerably with errors of 0.0046 and 0.0332 m/h in predicting normalized spread rates or equivalent no-wind no-slope non-adjusted spread rates respectively per unit error in LFMC. Fire spread rates for the southern rough fuel model show lesser sensitivity to live woody FMC than in pocosin. The sensitivity curves for southern rough also exhibit two different sensitivity regions, below 175 and above 175. When LFMC is below 175 in southern rough fuels, a unit error in estimating live woody fuel moisture may lead to an erroneous estimation of 0.0113 for normalized spread rates and 0.1668 m/h for the corresponding no-wind no-slope non adjusted spread rates. The corresponding errors when LFMC is above 175 are significantly smaller at 0.0015 and 0.0223 m/h. The uncertainty analysis for NDWI based LFMC retrievals revealed that 66% and 90% of LFMC estimation errors are expected to be below 32 and 56 respectively. We computed the errors in normalized spread rates and the no-wind-no-slope non adjusted spread rates for errors of 32 and 56 in LFMC retrievals to evaluate the implications of such errors in the predominant fuel models of Okefenokee. LFMC error estimates from NDWI based retrievals are only presented since they show less uncertainty than NDII. Interested readers can however easily calculate potential errors from NDII based retrievals.

4.3.1. Implication of LFMC retrieval errors in fuel model O

In pocosin fuel models, when the true LFMC is less than 100, errors of 32 and 56 in LFMC retrieval could lead to errors of 3.7 and 6.5 in normalized spread rates. This implies that at these low LFMC range predicted spread rates are expected to be within $3.7R_{125}$ and $6.5R_{125}$ of the actual spread rate (R_{125} is the spread rate at LFMC of 125 under similar conditions). Translating these results in terms of no-wind no-slope non adjusted spread rates would imply that at these low LFMC (≤ 100), the spread rate errors for 66% of cases are expected to be below 26.9 m/h while in 90% of cases, errors are expected to be below 47.1 m/h. However, when the actual LFMC is above 100, normalized spread rate errors decrease to 0.15 and 0.26 respectively for 66% and 90% of predictions, while the corresponding no-slope no wind non adjusted spread rate errors are 1.06 m/h and 1.86 m/h. It must be noted here that since the fire front progresses in all directions, small spread rate errors may eventually lead to substantial errors in burnt area predictions over a period of time. For example if a LFMC of 75 is retrieved as 100, a no-wind no slope non adjusted spread rate of 24.32 m/h will be wrongly estimated as 8.47 m/h. Under no wind no slope conditions, when the fire front progresses as concentric circles of increasing radii around the ignition point,

this spread rate error would lead approximately to an error of $\pi(24.38\times8)^2-\pi(8.47\times8)^2$ or around 10,5030 m^2 ($\sim$0.1 km^2) over a period of 8 h. In fire management perspective, this may be a considerable error considering that the USDA forest service designates a particular day as a "large fire day" on which a fire of final size over 10 acres ($\approx$0.04 km^2) (Andrews & Bradshaw, 1995) is discovered.

4.3.2. Implication of LFMC retrieval errors in fuel model D

In southern rough fuel models, when the actual LFMC is below 175, LFMC retrieval errors of 32 and 56 would result in errors of 0.36 and 0.63 for normalized spread rates and an equivalent 5.3 m/h and 9.3 m/h for no-wind no-slope non adjusted spread rates. At higher LFMC (>175) conditions, an error of 32 would propagate to an normalized spread rate error of 0.05 and no-wind no-slope non adjusted spread rate error of 0.71 m/h. At such wet conditions, an error of 56 would lead to corresponding errors of 0.08 and 1.25 m/h.

5. Conclusion

Empirical estimations of live fuel moisture content provide valuable information for fire risk estimation (eg Dasgupta et al., 2006) and the management of wild and prescribed fires. However, fire managers using them must be aware of the extent of the uncertainties involved in the empirical retrievals and how they can affect the accuracy of fire spread predictions. The objectives of this study were to estimate expected uncertainty ranges in empirical estimations of LFMC using NIR–SWIR spectral indices in the Okefenokee and to analyze the implications of these uncertainties for fire spread rate predictions. We have estimated the potential errors in remote sensing based LFMC estimations using two popular indices of NDWI $((R_{0.86}-R_{1.24})/(R_{0.86}+R_{1.24}))$ and NDII $((R_{0.86}-R_{1.64})/(R_{0.86}+R_{1.64}))$ and analyzed the implications of these errors in fire behavior predictions. The study was focused on the Okefenokee region in Georgia, USA. The results suggest that NDWI has a stronger linear relationship to LFMC than NDII and thus is expected to be a better estimator of LFMC. The better relationship of NDWI to LFMC can be attributed to the greater canopy penetration and less saturation at the weaker water absorption bands. Uncertainty analyses using simulated spectral indices were supported by studies using actual Aqua MODIS derived spectral indices for three Georgia Forestry Commission sites near Okefenokee, which had NFDRS model estimates of live woody FMC. Results show that LFMC retrieval errors using NDWI can be expected to be within 32 for 66% of retrievals and within 56 for 90% of retrievals. Errors are expected to be higher for regression models utilizing NDII. The effects of these LFMC retrieval errors on fire spread rate predictions were analyzed using the FARSITE fire behavior model. The sensitivity of fire spread rates to LFMC were determined from no-wind no-slope fire spread simulations on locally predominant fuel models O (high pocosin) and D (southern rough**)** under constant weather conditions**.** Sensitivity results were presented in terms of no-wind no-slope spread rates as well as normalized spread rates. Normalized spread rates, which are defined as the ratio of spread rate at a particular LFMC to the spread rate at LFMC of 125 under similar conditions, were used in order to make the results adaptable to any wind-slope conditions. Fire spread rates were observed to be very sensitive to live woody FMC below 100 for the pocosin fuel model and below 175 for the southern rough fuel model. For the pocosin fuel model under low LFMC conditions, (<100) errors of 56 (90% uncertainty limits) could lead to errors of 6.5 in normalized spread rates or an equivalent error of 47 m/h in predicting no-wind-no-slope non adjusted spread rates. In southern rough fuels for FMC below 175, errors of 56 in estimating LFMC could result in errors of 0.6 in normalized spread rates and an equivalent 9.3 m/h in predicting no-wind no-slope non adjusted spread rates. These spread rate error estimates represent approximately the upper bound of errors resulting from uncertainties from empirical retrievals of LFMC.

Error estimates obtained from our uncertainty analysis can be useful for other forested regions, where the variability in biophysical and biochemical leaf and canopy parameters are similar to the range of parameters used in the leaf and canopy radiative transfer model simulations. The results of this fire spread sensitivity analysis apply to the Okefenokee region where pocosin and southern rough fuels are predominant. However these fuel models are prevalent across the south eastern United States where our results can be applicable. Moreover they can serve as approximate results for other fuel models as well. Fire behavior prediction has typically utilized the 13 fuel models tabulated in Rothermel (1972) and Albini (1976). Anderson (1982) developed a similarity chart that allows mapping of NFDRS fuel models to the fire behavior fuel model of Rothermel. Based on this similarity chart, we can say that fire behavior in high pocosin is similar to fire behavior in mature bush (fuel model B), while fire behavior in southern rough resembles that in Alaska black spruce (fuel model Q), intermediate brush (fuel model F), sagebrush (fuel model T) and tundra (fuel model S). Owing to this similarity the present analysis may be applicable to fuel moisture retrievals in regions where the above mentioned fuel model types are present.

Acknowledgements

We would like to thank the anonymous reviewers and Dr. William Sommers (Director EastFIRE Lab, George Mason University) for their invaluable comments on improving this paper.

References

Albini, F. A. (1976). *Estimating wildfire behavior and effects.* General Technical Report INT-30: USDA Forest Service.

Alonso, M., Camarasa, A., Chuvieco, E., Cocero, D., Kyun, I., Martin, M. P., & Salas, F. J. (1996). Estimating temporal dynamics of fuel moisture content of Mediterranean species from NOAA-AVHRR data. *EARSeL Advances in Remote Sensing*, *4*, 9−24.

Anderson, H. E. (1982). Aids to determining fuel models for estimating fire behavior. *General technical report, INT 122.* Ogden, Utah: U.S.D.A. Forest Service, Intermountain Forest and Range Experiment Station.

Andrews, P. L. (1986). BEHAVE: Fire behavior predictions and fuel modeling system-BURN subsystem part I. *General technical report, INT-194* : U.S.D.A. Forest Service.

Andrews, P. L., & Bradshaw, L. S. (1995). Fire danger rating and the go/no-go decision for prescribed natural fire. *NFDRS reference CD.* Missoula, Montana: Fire Sciences Lab, U.S.D.A. Forest Service.

Bishop, G. N. (2000). *Native trees of Georgia.* Georgia Forestry Commission, tenth printing revised edition.

Bowyer, P., & Danson, F. M. (2004). Sensitivity of spectral reflectance to variation in live fuel moisture content at leaf and canopy level. *Remote Sensing of Environment*, *92*, 297−308.

Bradshaw, L. S., Deeming, J. E., Burgan, R. E., & Cohen, J. D. (1984). The 1978 National Fire Danger Rating System: Technical documentation. *General technical report INT-169.* Ogden, Utah: U.S.D.A. Forest Service, Intermountain Forest and Range Experiment Station.

Burgan, R. E. (1979). Estimating live fuel moisture for the 1978 National Fire Danger Rating System. *Research paper INT-226.* Ogden, Utah: USDA Forest Service, Intermountain Forest and Range Experiment Station.

Burgan, R. E. (1988). 1988 Revisions to the 1978 National Fire-Danger Rating System. *Research paper SE-273.* Asheville, North Carolina: U.S.D.A. Forest Service, Southeastern Forest Experiment Station.

Burgan, R. E., & Hartford, R. A. (1997). Live vegetation moisture calculated from NDVI and used in fire danger rating. In J. Greenlee (Ed.), *13th Conference on Fire and Forest Met., Lorne, Australia, Oct. 27–31, 1997.* Fairfield, Washington: IAWF.

Ceccato, P., Flasse, S., Tarantola, S., Jacquemond, S., & Gregoire, J. M. (2001). Detecting vegetation water content using reflectance in the optical domain. *Remote Sensing of Environment*, *77*, 22−33.

Ceccato, P., Flasse, S., & Gregoire, J. M. (2002b). Designing a spectral index to estimate vegetation water content from remote sensing data: Part 2. Validation and applications. *Remote Sensing of Environment*, *82*, 198−207.

Ceccato, P., Gobron, N., Flasse, S., Pinty, B., & Tarantola, S. (2002a). Designing a spectral index to estimate vegetation water content from remote sensing data: Part 1. Theoretical approach. *Remote Sensing of Environment*, *82*, 188−197.

Chuvieco, E., Deshayes, M., Stach, N., Cocero, D., & Riano, D. (1999). Short-term fire risk: foliage moisture content estimation from satellite data. In E. Chuvieco (Ed.), *Remote sensing of large wildfires in the European Mediterrranean Basin.* Berlin: Springer-Verlag.

Chuvieco, E., Riano, D., Aguado, I., & Cocero, D. (2002). Estimation of fuel moisture content from multitemporal analysis of Landsat thematic mapper. *International Journal of Remote Sensing*, *23*(11), 2145−2162.

Combal, B., Baret, F., Weiss, M., Trubuil, A., Mace, D., Pragnere, A., Myneni, R., Knyazikhin, Y., & Wang, L. (2002). Retrieval of canopy biophysical variables from bidirectional reflectance—using prior information to solve the ill-posed inverse problem. *Remote Sensing of Environment*, *84*, 1−15.

Cypert, E. (1961). The effects of fires in the Okefenokee swamp in 1954 and 1955. *American Midland Naturalist*, *66*, 483−503.

Dasgupta, S., Qu, J. J., & Hao, X. (2006). Design of a susceptibility index for fire risk monitoring. *IEEE Geoscience and Remote Sensing Society Newsletter*, *3*(1), 140−144.

Dennison, P. E., Roberts, D. A., Peterson, S. H., & Rechel, J. (2005). Use of Normalized Difference Water Index for monitoring live fuel moisture. *International Journal of Remote Sensing*, *26*(5), 1035−1042.

Dimitrakopoulas, A. P. (2002). Mediterranean fuel models and potential fire behavior in Greece. *International Journal of Wildland Fire*, *11*(2), 127−130.

Duever, M. J. (1971). Ecosystem analysis of Okefenokee swamp: Tree ring and hydroperiod studies, Okefenokee ecosystem investigations. *Technical report No 5.* Athens, Georgia: Institute of Ecology, University of Georgia.

Finney, M. A. (1998). FARSITE: Fire Area simulator — Model development and evaluation. *Research Paper, RMRS-RP-4.* Ogden, Utah: USDA Forest Service, Rocky Mountain Research Station.

Forest Service (1969). A Forest Atlas of the South: U.S.D.A.

Fourty, T., & Baret, F. (1997). Vegetation water and dry matter contents estimated from top-of-the atmosphere reflectance data: A simulation study. *Remote Sensing of Environment*, *61*, 34−45.

Gao, B. C. (1996). NDWI — A normalized difference water index for remote sensing of vegetation liquid water from space. *Remote Sensing of Environment*, *58*, 257−266.

Hardisky, M. A., Lemas, V., & Smart, R. M. (1983). The influence of soil salinity, growth form, and leaf moisture on the spectral reflectance of spartina alternifolia canopies. *Photogrammetric Engineering & Remote Sensing*, *49*, 77−83.

Hao, X., & Qu, J. J. (2007). Retrieval of real time live fuel moisture content using MODIS measurements.*Remote Sensing of Environment*, *108*, 130−137 (this issue). doi:10.1016/j.rse.2006.09.033.

Huemmrich, K. F. (2001). The GeoSail model: A simple addition to the SAIL model to describe discontinuous canopy reflectance. *Remote Sensing of Environment*, *75*, 423−431.

Huemmrich, K. F. (1995). An analysis of remote sensing of the fraction of absorbed photosynthetically active radiation in forest canopies. *Ph.D. Thesis*. University of Maryland.

Hunt, E. R., Rock, B. N., & Nobel, P. S. (1987). Measurement of leaf relative water content by infrared reflectance. *Remote Sensing of Environment*, *22*, 429−435.

Jackson, R. D. (1986). Remote sensing of biotic and abiotic plant stress. *Annual Review of Phytopathology*, *24*, 265−286.

Jackson, T. J., Chen, D., Cosh, M., Li, F., Anderson, M., Walthall, C., Doriaswamy, P., & Hunt, E. R. (2004). Vegetation water content mapping using Landsat data derived normalized difference water index for corn and soybeans. *Remote Sensing of Environment*, *92*, 475−482.

Jackson, R. D., Idso, S. B., Reginato, R. J., & Pinter, P. J. (1981). Canopy temperature as a crop water stress indicator. *Water Resources Research*, *17*, 1133−1138.

Jacquemoud, S. (1993). Inversion of the PROSPECT+SAIL canopy reflectance model from AVIRIS equivalent spectra: theoretical study. *Remote Sensing of Environment*, *44*, 281−292.

Jacquemoud, S., Bacour, C., Poilve, H., & Frangi, J. P. (2000). Comparison of four radiative transfer models to simulate plant canopies reflectance — Direct and inverse mode. *Remote Sensing of Environmnent*, *74*, 471−481.

Jacquemond, S., & Baret, F. (1990). PROSPECT: A model of leaf optical properties spectra. *Remote Sensing of Environment*, *34*, 75−91.

Jacquemoud, S., Baret, F., Andrieu, B., Danson, F. M., & Jaggard, K. (1995). Extraction of vegetation biophysical parameters by inversion of the PROSPECT+SAIL models on sugar beet canopy reflectance data. Application to TM and AVIRIS sensors. *Remote Sensing of Environment*, *52*, 163−172.

Jasinski, M. F., & Eagleson, P. S. (1989). The structure of red–infrared scattergrams of semivegetated landscapes. *IEEE Transactions on Geoscience and Remote Sensing*, *27*(4), 441−451.

Jasinski, M. F., & Eagleson, P. S. (1990). Estimation of subpixel vegetation cover using red–infrared scattergrams. *IEEE Transactions on Geoscience and Remote Sensing*, *28*(2), 253−267.

Kauth, R. J., & Thomas, G. S. (1976). The Tasseled Cap — Graphic description of the spectral–temporal development of agricultural crops as seen by Landsat. *Proceedings of the Symposium on Machine Processing of Remote Sensing Data* (pp. 41−51). West Lafayette: Purdue University.

Larcher, W. (1995). *Physiological plant ecology. Ecophysiology and stress physiology of functional groups*, (3rd ed.). New York: Springer, 528 pp.

Mitchell, K. A., Bolstad, P. V., & Vose, J. M. (1998). Interspecific and environmentally induced variation in foliar dark respiration among eighteen southeastern deciduous tree species. *Tree Physiology*, *19*, 861−870.

Montgomery, D. C., Peck, E. A., & Vining, G. G. (2001). Introduction to linear regression analysis. *Wiley Series in Probability and Statistics*, 37−39.

Moran, M. S., Clarke, T. R., Inoue, Y., & Vidal, A. (1994). Estimating crop water deficit using the relation between surface-air temperature and spectral vegetation index. *Remote Sensing of Environment*, *46*, 246−263.

Myneni, R. B., Nemani, R. R., & Running, S. W. (1997). Estimation of global leaf area index and absorbed PAR using radiative transfer model. *IEEE Transactions on Geoscience and Remote Sensing*, *35*, 1380−1393.

Nagler, P. L., Daughtry, C. S. T., & Goward, S. N. (2000). Plant litter and soil reflectance. *Remote Sensing of Environment*, *71*, 207−215.

Peñuelas, J., Filella, I., Biel, C., Serrano, L., & Save, R. (1993). The reflectance at the 950–970 nm region as an indicator of plant water status. *International Journal of Remote Sensing*, *14*, 1887−1905.

Peñuelas, J., Filella, I., Save, R., & Serrano, L. (1996). Cell wall elasticity and water index (R970 nm/R900 nm) in wheat under different nitrogen availabilities. *International Journal of Remote Sensing*, *17*(2), 378−382.

Peñuelas, J., Pinol, J., Ogaya, R., & Fillela, I. (1997). Estimation of plant water concentration by the reflectance Water Index WI (R900/R970). *International Journal of Remote Sensing*, *18*(13), 2869−2875.

Riano, D., Vaughan, P., Chuvieco, E., Zarco-Tejada, P. J., & Ustin, S. L. (2005). Estimation of fuel moisture content by inversion of radiative transfer models to simulate equivalent water thickness and dry matter content at leaf and canopy level. *IEEE Transactions of Geoscience and Remote Sensing*, *43*(4), 819−826.

Richards, G. D. (1990). An elliptical growth model of forest fire fronts and its numerical simulation. *International Journal of Numerical Methods Engineering*, *30*, 1163−1179.

Richards, G. D. (1993). The properties of elliptical wildfire growth for time dependent fuel and meteorological conditions. *Combustion Science and Technology*, *92*, 145−171.

Rothermel, R. C. (1972). A mathematical model for predicting fire spread in wildland fuels. *Research paper, INT-115.* Ogden, Utah: U.S.D.A. Forest Service, Intermountain Forest and Range Experiment Station.

Rothermel, R. C., Wilson, R. A., Morris, G. A., & Sacket, S. S. (1986). Modeling moisture content of fine dead wildland fuels: input to the BEHAVE fire prediction system. *Research paper, INT-359.* USDA Forest Service.

San-Miguel-Ayanz, J., Carlson, J. D., Alexander, M., Tolhurst, K., Morgan, G., Sneeuwjagt, R., & Dudley, M. (2003). Current methods to access fire danger potential. In E. Chuvieco (Ed.), *Wildland fire danger estimation and mapping, The role of remote sensing data* (pp. 21−61). Singapore: World Scientific Publishing Company.

Serrano, L., Ustin, S. L., Roberts, D. A., Gamon, J. A., & Peñuelas, J. (2000). Deriving water content of chaparral vegetation from AVIRIS data. *Remote Sensing of Environment*, *74*, 570−581.

Shipley, B., & Vu, T. T. (2002). Dry matter content as a measure of dry matter concentration in plants and their parts. *New Phytologist*, *153*, 359−364.

Trowell, C. T. (1987). *Some notes on the history of fire and drought in the Okefenokee swamp: A preliminary report. Working paper*, *Vol. 3*. Douglas, Georgia: South Georgia College.

Verhoef, W. (1984). Light scattering by leaf layers with application to canopy reflectance modeling: the SAIL model. *Remote Sensing of Environment*, *16*, 125−141.

Vidal, A., Pinglo, F., Durand, H., Devaux-Ros, C., & Maillet, A. (1994). Evaluation of a temporal fire risk index in mediterranean forests from NOAA thermal IR. *Remote Sensing of Environment*, *49*, 296−303.

Wang, L., Qu, J. J., Xiong, J., Hao, X., Xie, Y., & Che, N. (2006). A new method for retrieving band 6 of Aqua MODIS. *IEEE Geoscience and Remote Sensing Society Newsletter*, *3*(2), 267−270.

Yin, Z. (1993). Fire regime of the Okefenokee swamp and its relation to the hydrological and climatic conditions. *International Journal of Wildland fire*, *3*(4), 229−240.

Zarco-Tejada, P. L. J., Rueda, C. A., & Ustin, S. L. (2003). Water content estimation in vegetation with MODIS reflectance data and model inversion methods. *Remote Sensing of Environment*, *85*, 109−124.

Zarco-Tejada, P. L. J., & Ustin, S. L. (2001). Modeling canopy water content for carbon estimates from MODIS data at land EOS validation sites. *International Geoscience and Remote Sensing Symposium, 2001, (IGARSS'01)*, *I*, 342−344.